Chemical Engineering Journal 229 (2013) 498–507

Contents lists available at SciVerse ScienceDirect

Chemical Engineering Journal

journal homepage: www.elsevier.com/locate/cej

Dry torrefaction of biomass – Torrefied products and torrefaction kinetics using the distributed activation energy model

A. Sarvaramini, Gnouyaro P. Assima, F. Larachi *

Department of Chemical Engineering, Laval University, Québec, QC G1V 0A6, Canada

HIGHLIGHTS

- Thermogravimetric and fixed bed torrefaction of cellulose, xylan, lignin, aspen and birch.
- Biomass dehydroxylation and decarbonation reduce water uptake, H/C and O/C ratios.
- DAEM fits isothermal torrefaction kinetics of cellulose, hemicellulose and lignin.
- Torrefaction kinetics of woody samples is developed based on their constituents.

ARTICLE INFO

Article history:
Received 1 March 2013
Received in revised form 15 June 2013
Accepted 19 June 2013
Available online 27 June 2013

Keywords:
Lignocellulosic biomass
Torrefaction
Cellulose
Xylan
Lignin
Distributed activation energy model

ABSTRACT

Torrefaction is a thermal treatment applied to improve biomass properties for long-term storage and thermochemical conversion of wood. The torrefaction kinetic behavior of two woody biomass samples (aspen and birch) and their individual constituents (cellulose, xylan -hemicellulose proxy- and lignin) was studied in detail. The materials were torrefied in a fixed-bed reactor up to 280 °C and were characterized after 15 min and 60 min treatments in terms of their energy density, energy yield, H, O and C contents, humidity uptake and FTIR vibrational spectra. Regardless of mildness (240 °C) or severity (280 °C) of torrefaction, hemicellulose was the most reactive. Compared to torrefied cellulose, lignin exhibited considerable activity and increased heating value under severe torrefaction (280 °C). Likewise, the increase in heating value of torrefied cellulose was less significant than that of lignin due to cellulose energy loss because of production of tar compounds. The release of volatiles versus time for cellulose, xylan and lignin torrefaction reactions measured using a thermogravimetric method was also modeled for each lump by means of the distributed activation energy model and a three-parameter log-normal distribution function. The model was found to fit the experimental data for xylan and lignin torrefaction while it showed slight under-prediction in the case of cellulose torrefaction. The distributed activation energy models developed for the individual lumps were combined into a meta-model to apprehend the torrefaction kinetics of actual (aspen and birch) woody biomass by assuming parallel and independent involvement of their three constituents present under various compositions. The model was found to represent with very good agreement the experimental data of aspen and birch torrefaction.

© 2013 Elsevier B.V. All rights reserved.

1. Introduction

Environmental and economic constraints as well as resource scarcity are increasingly calling into question the classical fossil-energy driven development paradigm. In response, alternative solutions such as non-edible biomass are steadfastly climbing the ladder of the energy portfolio as potentially viable and perennial carbon neutral energy options [1,2]. However, as a fuel lignocellulosic biomass is disadvantaged in terms of O/C ratio, caloric value and moisture content, to name its main handicaps [3]. In order to upgrade biomass to a higher quality fuel, thermal treatments such as torrefaction are required. The goal behind torrefaction is to eliminate oxygen in the form of low caloric value torrefaction gases, e.g., CO_2, water and some organic acids, by exposing biomass to temperatures as high as 200–300 °C [4–6]. In spite of the fact that *ca.* 30 wt.% of biomass is lost during torrefaction the recovered solid may retain up to 90% of the initial biomass energy content [3]. In comparison to the parent raw biomass, torrefied solid products should bear certain properties such as lower moisture content, lower O/C ratio, and higher energy density to make them suitable biofuels [4–6].

Different torrefaction processes, e.g., dry torrefaction [4–6], wet torrefaction [7,8] and ionic-liquid assisted torrefaction [9] have been proposed to leverage the above biomass properties. Dry torrefaction consists of slow heating of biomass in an inert

---

* Corresponding author. Tel.: +1 418 656 3566; fax: +1 418 656 5993.
E-mail address: faical.larachi@gch.ulaval.ca (F. Larachi).

1385-8947/$ - see front matter © 2013 Elsevier B.V. All rights reserved.
http://dx.doi.org/10.1016/j.cej.2013.06.056

atmosphere from 200 °C to 300 °C [4–6,10]. During this treatment, the three main constituents of biomass, i.e., hemicellulose, cellulose and lignin [11] decompose at different rates. Hemicellulose is the most sensitive lump to be affected by dry torrefaction unlike cellulose whose decomposition is the rate limiting step of torrefaction [12]. The rate of cellulose decomposition is stimulated by elevated torrefaction temperatures, though temperatures in excess of 300 °C are not recommended due to the release of heavy tars which tendency is to reduce biomass energy density [12]. Impregnation of biomass with room-temperature ionic liquids enhanced the rate of cellulose torrefaction at temperatures lower than 300 °C [9]. However, despite advantages showcased by ionic liquids, the solid products resulting from ionic-liquid torrefaction treatments still require further improvements such as energy yield which was found to be lesser compared to the dry-torrefaction analogs [9]. In addition, cost of ionic liquids should be factored in if such advanced approaches are to be sought for commercial applications of biomass torrefaction [13]. Wet torrefaction or hydrothermal pretreatment of biomass performed in a pressurized liquid water up to 5 MPa and 260 °C produces solids with energy density greater than that obtained from dry torrefaction [7,8]. Likewise, elevated pressures tend to reflect in increased operational costs also. Therefore, it is likely that dry torrefaction, because of its rustic character and low cost, will still encompass the majority of lignocellulosic biomass torrefaction units [14].

Several kinetic models have been proposed for biomass torrefaction in dry inert atmosphere which are mostly of pseudo-mechanistic nature where one or several pseudo-reactions are assumed for modeling biomass torrefaction [12,15,16]. We are of the opinion that the wide range of heterogeneous reactions taking place during torrefaction must call for more appropriate mathematical representations. These latter must be able to account for the distributed nature of the reactions across the biomass structure, e.g., catalytic effects of the alkali metals, and the corresponding wide range of activation energies [17] which are not reflected in current models. We propose to evaluate the potential of the distributed activation energy model (DAEM) which is viewed as one of the most accurate approaches for modeling biomass pyrolysis [17]. The model assumes an infinite number of irreversible *n*th-order parallel reactions with different activation energies occurring simultaneously and where the difference in activation energies is represented by a distribution function. The DAEM has been widely used to analyze complex reactions such as pyrolysis of various ranks of coal and other fuels [18–21]. Yet, and to the best of the authors' knowledge, the merit of using DAEM has not been assessed for representing biomass torrefaction kinetics.

This work, therefore, aims at studying the dry torrefaction properties and kinetics of the main biomass constituents, i.e., xylan (hemicellulose proxy), cellulose and lignin, as well as two different hardwoods, i.e., aspen and birch. Characterization experiments were designed such that they evaluate a number of properties which are of paramount importance in the field of biomass torrefaction and provide a rather consolidated study. To do so, the main biomass constituents, birch and aspen were torrefied under mild and severe torrefaction conditions and the contribution of each biomass constituents on the properties of torrefied biomass was analyzed by obtaining their heating value and energy yield. Major emphasis was put on lignin which is considered as an inert compound in some existing literature [22,23] and thus its decomposition rate, heating value and energy density of torrefied lignin was compared with that of cellulose. The FTIR analysis performed on the raw and torrefied samples also helped gaining an understanding on the mechanism of cellulose, hemicellulose and lignin torrefaction. Moreover, the humidity uptake of each biomass constituents subjected to the mild and severe torrefaction conditions was studied to investigate their impact on equilibrium moisture content of torrefied birch and aspen. Finally, a DAEM kinetic model for the torrefaction of each constituent, separately, and for both hardwood samples is formulated. To achieve this, separate DAEM models are developed for each one of hemicellulose, cellulose and lignin lumps by monitoring their thermal decomposition rates versus time in a torrefaction environment using a thermogravimetric analyzer (TG). The quality of the models is judged both by their predictive power for actual wood samples using recombined kinetics from the constitutive wood lumps and actual torrefaction kinetics of aspen and birch samples.

2. Experimental

Isothermal torrefaction studies were carried out using trembling aspen and birch, two abundant woody biomass samples from Québec forests (Canada), as well as powdered samples of cellulose (Avicel®PH-101), xylan (X0502) and lignin (37,059-lignin, alkali), all three purchased from Sigma Aldrich. The proximate and ultimate analyses of the studied samples are summarized, respectively, in Tables 1 and 2. The birch and aspen samples were first grinded and then sieved to isolate particles finer than 500 μm. The samples were then torrefied in a fixed-bed torrefaction reactor. The bench scale biomass torrefaction unit consisted of a stainless steel (SS) fixed-bed reactor (ID. 34 mm, length 70 cm) placed inside an induction coil. For each one of the experiments, 300 mg of biomass was held atop of a steel grid located in the middle of a stainless steel tube to act as a support for the biomass bed. The reactor was heated through a 30 cm long coil connected to a 18 kW induction power supply for heating the stainless steel tube *via* an AC magnetic field then heating in turn the biomass layer through radiation and conduction. The biomass bed temperature was raised from the ambient to the target temperature (240 °C and 280 °C) in less than 10 s and then the samples were kept at the final temperature for specified time durations, 15 and 60 min, respectively. These torrefaction temperatures, i.e., 240 °C and 280 °C were representatives of mild and sever torrefaction conditions, respectively [24]. The SS tube temperature was controlled by a fiber optic pyrometer connected to a temperature controller to meter the induction-heater power. Temperature was also measured through a K type thermocouple inserted in the center of the biomass bed. The difference in temperature between the bed and SS tube surface never exceeded 5 °C in steady-state conditions. Volatiles forming in the reactor were directed towards a cold trap by sweeping the bed with a continuous N_2 flow (200 N mL/min).

The solid products obtained after torrefaction were further analyzed to quantify their properties after thermal treatment. The solid products were weighted to obtain their mass yield (Y_M = %mass solid product/mass feed) after torrefaction. The C, H, N, S contents of the samples were also measured using an elemental analyzer (Fisons EA 1108CHNS). All measurements were repeated twice and their averages were reported. The higher heating value (HHV) of the samples before and after torrefaction were determined using a relationship obtained by Channiwalaet al. [25] based on carbon, hydrogen, oxygen, sulfur, nitrogen and ash content of biomass. The model developed in their work was tested for 225

Table 1
Proximate analysis in mass% of cellulose, xylan, lignin, birch and aspen wood.

	Humidity	Volatile (dry basis)	Fixed carbon (dry basis)	Ash (dry basis)
Cellulose	3.4	93.1	6.9	<0.1
Xylan	8.5	74.2	24.7	1.1
Lignin	3.1	49.3	47.5	3.2
Birch	5.5	89.4	9.8	0.7
Aspen	4.8	87.5	12	0.5

Table 2
Ultimate analysis, O/C and H/C mole ratio, mass yield, high heating value, energy yield and energy density of as received and torrefied cellulose, xylan, lignin, birch and aspen.

	C	H	N	S	O	O/C mole ratio	H/C mole ratio	Mass yield (%)	Energy yield	HHV (kJ/g)	Energy density ratio
Cellulose											
Raw	42.8	6.4	0	0	50.8	0.89	1.81	···	100	17.3	1
Torrefied at 240 °C	43.6	6.3	0	0	50.1	0.86	1.72	98.1	98.8	17.4	1.0
Torrefied at 280 °C	44.4	6.2	0	0	49.4	0.83	1.69	90.1	92.5	17.7	1.03
Xylan											
Raw	40.4	6.1	0	0	53.4	0.99	1.82	···	100	15.5	1
Torrefied at 240 °C			0	0		0.51	0.92	54.5	71.2	20.2	1.31
Torrefied at 280 °C	56.7	4.4	0	0	38.9	0.44	0.81	41.2	56.0	21.0	1.36
	60.4	4.1			35.5						
Lignin											
Raw	63.7	6.0	0.90	2.29	27.2	0.32	1.13	···	100	25.6	1
Torrefied at 240 °C						0.24	0.95	89.9	96.6	27.7	1.07
Torrefied at 280 °C	69.5	5.5	0.60	2.12	22.2	0.23	0.93	87.3	94.8	28.0	1.09
	70.6	5.5	0.60	1.99	21.4						
Aspen											
Raw	47.0	6.2	0.01	0	46.7	0.74	1.60	···	100	18.9	1
Torrefied at 240 °C				0		0.66	1.46	86.4	91.6	20.0	1.06
Torrefied at 280 °C	50.0	6.1	0.02	0	43.9	0.62	1.36	78.5	84.90	20.4	1.08
	51.6	5.9	0.02		42.50						
Birch											
Raw	47.6	6.1	0.05	0	46.3	0.73	1.54	···	100	18.9	1
Torrefied at 240 °C				0		0.63	1.40	86.2	92.3	20.2	1.07
Torrefied at 280 °C	51.0	6.0	0.06	0	43.0	0.59	1.28	74.5	81.5	20.6	1.09
	52.9	5.7	0.09		41.4						

samples and was shown to be applicable for estimation of the high heating values of torrefied biomass [26,27]:

$$\mathrm{HHV}\ (\mathrm{kJ/g}) = 0.3491 \times C + 1.1783 \times \mathrm{H} + 0.1005 \times \mathrm{S} - 0.1034 \times \mathrm{O} - 0.0151 \times \mathrm{N} - 0.0211 \times \mathrm{Ash}$$

With C, H, S, O, N and Ash representing carbon, hydrogen, sulfur, oxygen, nitrogen and ash mass percentages, respectively. Using the solid product HHV, the energy density (e = HHV solid product/HHV feed) and energy yield ($Y_e = e \cdot Y_M$) of the solids were also obtained.

To investigate the effect of torrefaction on the samples hydrophobicity, equilibrium moisture content (EMC) analysis was also performed on the torrefied samples. EMC of raw and torrefied biomass samples were obtained by putting 300 mg samples in a vapor-saturated environment controlled at 25 °C. All the samples were oven-dried at 110 °C overnight to remove the pre-existing humidity in the samples before EMC analysis. The samples weight gain was measured after ten days which was estimated to be enough for the samples to reach moisture equilibrium uptake. Fourier transform infrared spectroscopy (FTIR) (Nicolet Magna 850 spectrometer, Thermo Scientific, Madison, WI) was also performed on the as-received and torrefied cellulose, xylan and lignin to study changes in their functional groups during torrefaction. The FTIR was equipped with high temperature Golden Gate ATR accessory.

For the derivation of the kinetic model for biomass torrefaction, isothermal torrefaction kinetics of all five substrates were performed in a thermogravimetric analyzer (TG) (Perkin Elmer Lab System Diamond TG–DTA) used to monitor the weight loss of the samples during torrefaction. TG is appropriate for developing kinetic models for steady-state (isothermal) or low-heating rate biomass torrefaction [28]. For this purpose, the samples were placed in an alumina ceramic holder forming a small bed with initial mass of 5–8 mg of woody biomass, lignin, cellulose, or xylan. The samples were first dried in TG at 120 °C for 15 min and then heated up to the target temperature (240–290 °C) with the maximum achievable heating rate (~200 °C/min) under N_2 flow (200 N mL/min). The isothermal torrefaction of the samples was performed by maintaining the samples at the target temperature between 15 and 180 min while samples' mass was adjusted so that weight losses during torrefaction never dived below 30 wt.%.

3. Kinetic modeling

The total amount of volatiles released during torrefaction of xylan, lignin and cellulose were modeled separately using DEAM from the mass loss registered *via* TG. In this model, the decomposition of xylan, lignin and cellulose during torrefaction is considered to result from an infinite number of n th-order parallel reactions. For a particular ith reaction decomposition rate, one has:

$$\frac{\mathrm{d}(V_i/V_i^*)}{(1 - V_i/V_i^*)^n} = k_i \mathrm{d}t \quad (1)$$

where "i" may contribute to the decomposition of xylan, lignin and cellulose. In Eq. (1), V_i refers to the volatile contribution from reaction "i" during torrefaction of each biomass model compound and V_i^* denotes the maximum volatile contribution to be released due to reaction "i". The rate constant of reaction "i" is expressed following an Arrhenius form as:

$$k_i = A_i \exp(-E_i/RT) \quad (2)$$

In which R is the universal gas constant, A_i is the frequency factor, E_i is the activation energy and T is the torrefaction temperature. Considering that the number of parallel reactions during the torrefaction of each compound is infinite, the maximum volatile contribution released by each reaction (V_i^*) can be considered as a fraction of the total volatiles (V^*) with activation energies between E_i and $E_i + \delta E_i$, i.e., $V_i^* = V^* f(E_i)\delta E_i$). Consequently, the total volatiles evolved up to time instant t during torrefaction of each compounds can be expressed as [29]:

$$\frac{V^r}{V^*} = 1 - \frac{V}{V^*} = \int_0^\infty f(E)[1 - (1-n)\int_0^t A\exp(-E/RT)dt]^{1/1-n} \mathrm{d}E \quad (3)$$

In Eq. (3), $f(E)$ is the distribution of activation energies ($\int_0^\infty f(E)\mathrm{d}E = 1$), V is the amount of volatiles evolved up to time t, V^* is the maximum volatile content of each compound and V^r is the residual compound volatile which is not released. In the special case where the order of the reaction is equal to one, Eq. (3) reduces to:

$$\frac{V^r}{V^*} = 1 - \frac{V}{V^*} = \int_0^\infty f(E)e^{-\int_0^t A\exp(-E/Rt)dt}\mathrm{dE} \tag{4}$$

Several probability density functions such as Gaussian [18,29], Weibull [30,31] and Gamma [32] distributions have been tested for biomass pyrolysis. In the present study, the three -parameter log-normal distribution was used to model the distribution of activation energies of cellulose, xylan and lignin during torrefaction.

$$f(E) = \frac{1}{(E-E_0)\sqrt{2\pi}\delta}\exp\left\{-\frac{(\ln(E-E_0)-\mu)^2}{2\sigma^2}\right\} \quad \text{for} \quad E > E_0$$
$$f(E) = 0 \quad \text{for} \quad 0 < E < E_0 \tag{5}$$

Substituting $f(E)$ in Eqs. (3) and (4) by a log-normal distribution function leads to a double integral for which there is no analytical solution. Alternatively, numerical methods such as recursive adaptive Simpson quadrature technique available in MATLAB were used. There are five unknown parameters in the torrefaction DAEM for cellulose, lignin and xylan, i.e., μ, δ and E_0 being the unknowns in the log-normal distribution and n and A associated with the order and frequency factor. These torrefaction kinetic parameters were obtained using a simulated annealing optimization technique. This technique is a derivative-free optimization method recommended for finding global optima for DAEM [33].

The DAEM developed for the isothermal torrefaction of cellulose; xylan and lignin could be employed to develop a kinetic model for the torrefaction of aspen and birch. It is assumed that the aspen and birch torrefaction is the result of torrefaction of their constitutive cellulose, xylan and lignin in a way that there is no interaction between components. Consequently, the following equation can be written to relate the torrefaction of aspen and birch at time t to the torrefaction of their main constituents.

$$(V/V^*)_{total} = \sum_{i=1}^{3} c_i(V/V^*)_i \tag{6}$$

In Eq. (6), c_i represents the contribution of each compound to the total volatiles release. Using the simulated annealing optimization technique, the optimum values of c_i which could fit the three component model to the experimental torrefaction data of aspen and birch could be obtained.

4. Results and discussion

4.1. Biomass torrefaction

Lignin torrefaction. Lignin is a stable biopolymer which confers rigidity and strength to cellulose in the plant cell wall [34]. It consists of different proportions of guaiacyl (G), *p*-hydroxyphenyl (H) and syringyl (S) units which are inter-bonded irregularly through different types of linkages; the so-called βO_4 linkage being the most frequent one [35–37]. Lignin resistance to decomposition depends on the type of linkages between its building units [36]. The aryl ether linkages (C—O—C) have low disassociation energy while the biphenyl type linkages are more resistant to breakage [36]. Lignin decomposition takes place at temperatures as low as 150 °C, earlier than xylan and cellulose though at quite a tepid rate (Fig. 1). Lignin decomposition rate increases slowly with temperature until 300 °C and reflects in a slight decrease in solids mass yield by increasing the torrefaction temperature (Table 2). For instance, lignin torrefaction at 240 °C and 280 °C led, respectively, to 89.9% and 87.3% of dry mass yield. The lignin torrefaction is slightly exothermic as can be observed in Fig. 1.

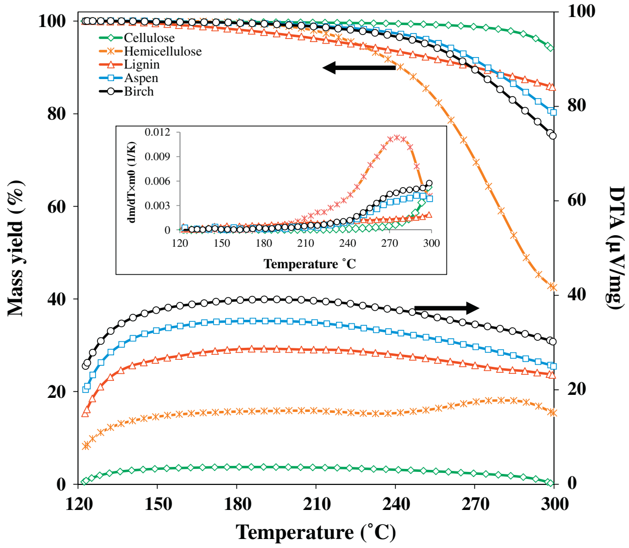

Fig. 1. Mass yield, weight loss derivative and differential thermal analysis of cellulose, xylan, lignin, birch and aspen wood decomposed in thermogravimetric analyzer at 5 °C/min heating rate until 300 °C.

Torrefaction reduces the O/C and H/C atomic ratios in lignin (Table 2). As an example, these ratios are reduced from H/C = 1.12 and O/C = 0.32 in raw lignin to H/C = 0.93 and O/C = 0.23 for lignin torrefied at 280 °C. Also, these ratios are sensitive to torrefaction temperature such that the lignin carbon content increases with increasing the torrefaction temperature, whereas those of oxygen and hydrogen decrease. Reduction in O/C and H/C ratios can also be expected from the analysis of lignin decomposition volatiles at temperatures lower than 300 °C. The release of H_2O, CO_2, formaldehyde and formic acid with higher O/C and H/C ratios than raw lignin, as a result of the cleavage of OH and carbon groups in the alkyl side chains, explains indeed these ratios' trends in torrefied lignin [36]. The energy density of torrefied lignin at 240 °C and 280 °C increases by 7% and 9% (on a dry basis), respectively, due to the reduction in the oxygen content of lignin (Table 2). Considering that almost 3% of raw lignin consists of water, the energy density of torrefied lignin improves by *ca.* 10% with respect to that of untreated lignin. Lignin mass loss amounts to 13–17% due to

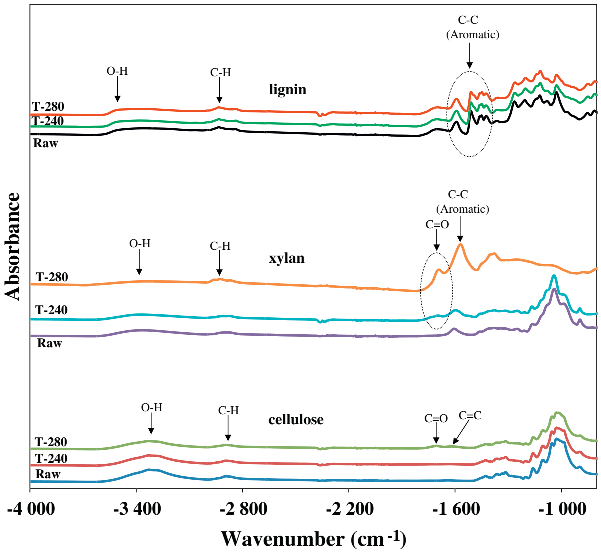

Fig. 2. FTIR spectra of as-received and torrefied cellulose, xylan and lignin samples.

torrefaction treatment while almost 95% of its energy is preserved in the torrefied lignin product (Table 2). According to the van Krevelen diagram, raw lignin shares the fuel characteristics of low rank coals such as lignite or sub-bituminous coal [3].

Lignin FTIR spectra before and after torrefaction at 240 °C and 280 °C are shown in Fig. 2. The aromatic nature of lignin due to the guaiacyl (G), *p*-hydroxyphenyl (H) and syringyl (S) units manifests in the vibrational range of 1400–1600 cm^{-1} due to the C—C bonds in the aromatic structure [35]. Likewise, both aliphatic and phenolic hydroxyl groups, which prompt hydrogen bonding in the lignin polymeric structure, exhibit a broad hydroxyl peak in the 3200–3600 cm^{-1} range [38]. Though torrefaction promotes lignin dehydroxylation and thus a reduction in the extent of hydrogen bonding, such changes are barely visible in terms of broadness and relative of OH vibrational peaks in the FTIR spectra of the torrefied lignin (Fig. 2). Lignin torrefaction leads to a decrease in the peak intensities near 1035, 1205 and 1265 cm^{-1} which are assigned to C—O bond deformations in methoxyl groups, C—O bond stretching in phenolic hydroxyl groups and C—O bond stretching in the ether aromatics, respectively [35].

Torrefaction reduces the equilibrium moisture content of lignin as well. The major mechanism for water adsorption on lignin is water physisorption *via* hydrogen bonds between water and the free hydroxyl groups in the lignin subunits [39]. Torrefaction also leads to a partial destruction of the free hydroxyl groups in the lignin. This translates in almost 40% reduction in equilibrium moisture uptake of treated lignin as shown in Fig. 3 Increasing the torrefaction temperature could extend the lignin dehydroxylation causing less water uptake by lignin.

Cellulose torrefaction. Cellulose consists of linear chains of several hundreds to thousands of $\beta(1 \rightarrow 4)$ linked D-glucose units [40,41]. Cellulose decomposition commences around 260 °C with a rate that increases with temperature (Fig. 1). Similar to lignin, the torrefaction of cellulose is slightly exothermic. Torrefaction of cellulose at mild and severe conditions led to 1.9% and 9.9% mass reduction as can be seen in Table 2. The lower mass yield of torrefied cellulose at mild and severe conditions in comparison with lignin shows its lower rate of decomposition than lignin in the torrefaction temperature range. The mass reduction of mild condition torrefied cellulose is considerably lower than that of torrefied lignin at the same torrefaction conditions (1.9% and 10.1%, respectively). Although cellulose decomposition at mild condition torrefaction was low, a reduction in H/C and O/C ratios in cellulose was observed (Table 2). The mild torrefaction led to the reduction in the H/C and O/C ratios of cellulose from H/C = 1.81 and O/C = 0.89 in raw cellulose to H/C = 1.72 and O/C = 0.86 in the mild condition torrefied cellulose. The decrease in the H/C and O/C ratios of mild condition torrefied cellulose could be due to the intra-molecular elimination of water from the torrefied cellulose. Due to the reduction in the O/C and H/C of torrefied cellulose, the energy density of mild condition torrefied cellulose was increased by 1%. In the case of severe condition torrefied cellulose, the mass yield of torrefied cellulose was more comparable with that of torrefied lignin in the same conditions (90.1% and 87.3%, respectively, Table 2). However, the increase in carbon content of torrefied lignin at the same conditions is quite higher than that of cellulose (10.8% and 3.7%, respectively). The same trend was also observed for the oxygen and hydrogen content of torrefied cellulose and lignin at severe torrefaction condition. The reduction in oxygen and hydrogen content of severe condition torrefied cellulose were 2.75% and 3.13% while oxygen and hydrogen content of lignin reduced by 21.3% and 8.3%, respectively. These results indicate that the severe condition torrefaction of cellulose leads to the loss of some carbon in the form of tar. The release of tar could be the main reason for the small increase in the energy density of severe condition torrefied cellulose than lignin. Although some previous torrefaction studies [22,23] indicated that lignin is relatively inert under torrefaction conditions, these results reveal some activity which might not be neglected in comparison to that of cellulose at equal temperature and treatment time.

FTIR spectra of the as-received cellulose and the torrefied cellulose at 240 °C and 280 °C are shown in Fig. 2. The changes in the FTIR spectrum of torrefied cellulose at 280 °C (severe treatment) is more pronounced than that for 240 °C (mild treatment). However, the cellulose main vibrational features are still perceptible after torrefaction. Cellulose torrefaction at 280 °C leads to partial dehydroxylation reflecting in decreased intensities of the vibrational peak at 3200–3400 cm^{-1} (O—H stretching) and 2850–2950 cm^{-1} (C—H stretching). The FTIR spectrum of torrefied cellulose at 280 °C pinpoints to the inception of two new peaks at 1620 cm^{-1} and 1705 cm^{-1} attributed, respectively, to unsaturated carbon–carbon (C═C) and carbonyl (C═O) stretching bonds. The dominant mechanism for cellulose decomposition at torrefaction temperatures below 300 °C occurs *via* cellulose dehydration [42].

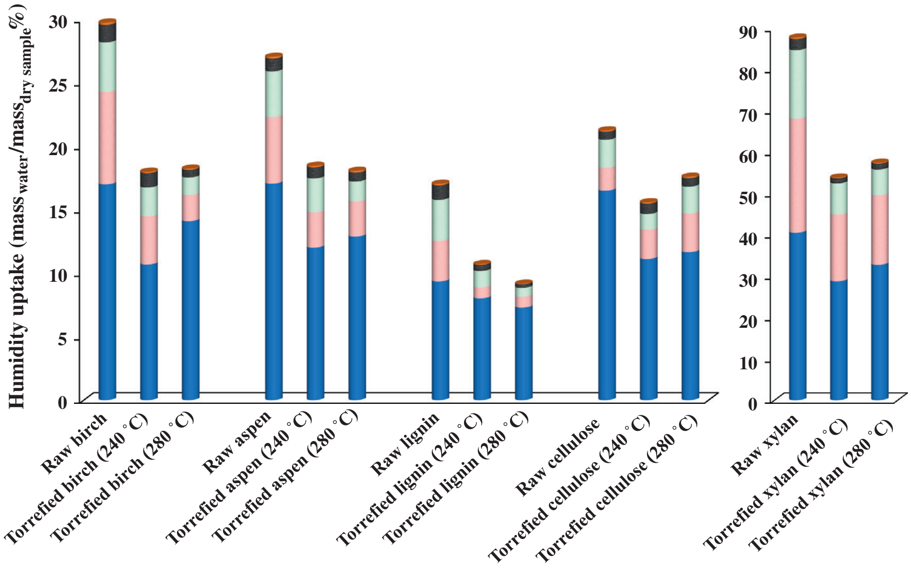

Fig. 3. Humidity uptake of the as-received and torrefied cellulose, xylan, lignin, birch and aspen wood at 25 °C during 5 intervals of 48 h.

Intramolecular elimination of water from pyranose-ring C_2 and C_3 carbons leads to unsaturated pyranose rings (enol-anhydrocellulose) recognizable from the incipient vibrationals peaks at 1705 cm^{-1} as well as formation of ketone species (keto-anhydrocellulose) as revealed by 1620 cm^{-1} peak [42]. However, at torrefaction temperatures over 250 °C, in addition to dehydration reactions, cellulose degradation could also cause the formation of some levoglucosan (tar), CO, CO_2 and some acid hydrocarbons [43]. Cellulose torrefaction favors loss of polar hydroxyl groups leading to thus to lesser water adsorption *via* hydrogen bonding. This is confirmed from Fig. 3 where nearly 30% reduction in equilibrium moisture content of torrefied cellulose was noted in comparison to moisture uptake of raw cellulose.

Hemicellulose torrefaction. After cellulose, hemicellulose is the most abundant polysaccharide group in plant [44]. Depending on its source, it could contain different sugar monomers such as glucose, xylose, mannose, galactose, rhamnose and arabinose [45,46]. According to the type of sugar residues, hemicellulose species are grouped into four classes such as xylans, xyloglucans, and mannose and mixed-linkage β-glucans [47]. Each class could be also divided into several subgroups depending on the type and chemical nature of the side chains in their structure. Hardwood hemicellulose is mainly composed of xylan which has a linear polymeric skeleton form constituted of 1–4 liked β-xylano pyranosyl units which could be substituted by O-methyl-D-glucuronic acid residue [48]. The acetyl groups could also substitute the side chains in the xylanopyranosyl units [48,49].

Xylan decomposition initiates at temperatures around 200 °C. This temperature is lower than that of cellulose but higher than that of lignin (Fig. 1). The lack of crystallinity and lower polymerization degree of hemicellulose as compared to cellulose could lead to less thermal and chemical stability for hemicellulose [49]. The rate of xylan decomposition increases with temperature up to a maximum near 280 °C (Fig. 1). Therefore, temperatures lower than 300 °C are suitable for xylan torrefaction. Xylan torrefaction under mild and severe conditions also led to mass losses, respectively, 45.5% and 58.8% (Table 2). These levels are considerably higher than those of lignin and cellulose for the same torrefaction conditions. It can be concluded that hemicellulose is the component most sensitive to torrefaction treatments. Xylan energy losses due to mild and severe torrefaction represent some 28.9% and 44.1%, respectively (Table 2). These loss percentages are lower than the corresponding mass loss percentages in the same conditions. The high oxygen concentration in xylan lowers its energy density and thus its higher heating value. However, torrefaction reduces oxygen concentration in xylan and eventually increases its energy density. The loss of oxygen from xylan upon torrefaction could also be the reason for its slight exothermic decomposition (Fig. 1). The H/C and O/C ratios decreased, respectively, from 1.82 and 0.99 in the as-received xylan to 0.92 and 0.51 (mild treatment) and to 0.81 and 0.44 (severe treatment). This was mirrored by an increase of 1.3% and 1.4% of energy density of torrefied xylan, respectively, for the mild and severe treatments.

The FTIR spectra of as-received and torrefied xylan are shown in Fig. 2. It can be seen that xylan torrefaction at mild conditions could not complete the transformation xylan chemical structure. Xylan decomposition at temperatures lower than 250 °C is known to be preceded by the release of water, CO, CO_2, methanol, aldehyde type and acetic products [48]. The peak at 1690 cm^{-1} assigned to carbonyl (C=O) functional groups in the torrefied xylan is a marker to follow the progress of xylan decomposition at 240 °C. However, xylan torrefaction at 280 °C (severe conditions) leads to major changes in xylan FTIR spectrum (Fig. 2). Decomposition of xylan at 280 °C is believed to lead to cleavage of glycosidic residues and release of furfurals, acids, water and other gases [48]. Peak intensities in the ranges 950–1200 cm^{-1} (simple C—O bond stretching) and 3200–3600 cm^{-1} (simple O—H bond stretching) decrease considerably upon treatment indicating a loss of these groups. This is unlike the intensity of C=O bond (1690 cm^{-1}) which increased due to torrefaction at 280 °C. Likewise, xylan carbonization during torrefaction and loss of hydrogen and oxygen led to the formation of aromatics (peaks at 1570 cm^{-1}) as also confirmed by the spectral upward drift towards the large-wave number region [50].

Fig. 3 shows that the moisture uptake by as-received xylan is considerably larger than that of cellulose and lignin. In addition to the presence of polar hydroxyl and carboxyl groups, the amorphous structure of xylan enhances the adsorption of water in comparison with cellulose. Upon torrefaction treatment, dehydroxylation and decarboxylation of xylan could lead to a considerable decrease in equilibrium moisture content. The equilibrium moisture content of torrefied xylan at 240 °C and 280 °C is 38% and 35% less than that of non-treated xylan.

Birch and aspen torrefaction. Thermal decomposition of aspen and birch, as shown in Fig. 1, started at a temperature as low as 180 °C likely *via* lignin decomposition. As discussed earlier, lignin decomposition took place at temperatures as low as 150 °C. The rate of aspen and birch decomposition slightly increased from *ca.* 200 °C after decomposition of hemicellulose in birch and aspen was initiated, Fig. 1. Torrefaction of aspen and birch also exhibits a similar exothermic behavior as expected from the individual exothermic behaviors of their constituents.

Results of elemental analysis as well as mass and energy yields of severe and mild torrefaction of aspen and birch are summarized in Table 2. The mild torrefaction of birch and aspen woods led to the respective mass yields of 86.2% and 86.4%. Increasing the torrefaction temperature also decreased the mass yield of torrefied birch and aspen to the respective values of 74.5% and 78.5%. The considerable decrease in mass yield of torrefied birch and aspen by increasing the torrefaction temperature was expected as the main constituents of birch and aspen such as cellulose, hemicellulose and lignin also showed the same trends due to torrefaction. As can be observed in this table, the H/C and O/C ratios of torrefied birch and aspen reduced substantially due to the torrefaction at mild and sever conditions. These reductions in H/C and O/C ratios of mild condition torrefied birch and aspen led to 7% and 6% increase in their energy density ratio, respectively. Although birch and aspen are only losing around 14% of their mass, the increase in their energy density is significant. At severe torrefaction conditions, the weight loss of birch and aspen increased to 25.5% and 21.5%, respectively, but their energy density slightly increased about 9% and 7%, respectively, with respect to the non-treated wood samples. This trend could be explained due to the presence of high amounts of cellulose in the structure of birch and aspen woods. Almost 58.9% and 51.2% of birch and aspen wood are composed of cellulose [51,52]. As observed during torrefaction of cellulose; the severe condition torrefaction of cellulose leads to release of some tar compounds such as levoglucosan [43] due to its rapid decomposition causing energy loss during torrefaction. Consequently, although the mass yields of severe condition torrefied birch and aspen woods are much lower than those of mild condition torrefied birch and aspen, the difference in their energy density is not that noticeable.

The equilibrium moisture content of torrefied aspen and birch is reduced by 30% due to torrefaction, Fig. 3. This trend was expected from investigation of the individual biomass constituents. The loss of some biomass polar groups such as hydroxyl and carboxyl groups during torrefaction is the main reason for the observed behavior. The equilibrium moisture content of the as-received aspen and birch was 30% and 26%, respectively. Torrefaction reduced its level to 17% for both wood samples. Torrefaction as a strategy to improve resistance to fungal colonization correlates with the reduction of equilibrium moisture content of the treated wood. Since fungal growth on lignocellulosic materials is strongly correlated to water uptake [53]. A significant wood decomposition was reported to occur above the wood fiber saturation point at 25–35% moisture content [54]. It should be mentioned that limited biomass decomposition due to fungal growth may also occur at moisture levels as low as 20% [55]. Certain types of fungi such as Aspergillus and Penicillium could grow at biomass moisture contents below 15% [56]. Hence, attenuation of microbiological activity in torrefied wood could facilitate its long-time storage.

4.2. Kinetic modeling of torrefaction

In the following section, first a DAEM was developed for the torrefaction of the individual components, cellulose, xylan and lignin. The DAEM parameters for each compound was optimized so that the model fits the TG mass loss profile for each compound versus time at three different torrefaction temperatures, 240 °C, 260 °C and 280 °C. The DAEM optimal parameters for xylan, lignin and cellulose as gathered in Table 3. Furthermore, the DAEM was tested for predicting the TG mass loss profiles of torrefied xylan, lignin and cellulose versus time measured at 250 °C, 270 °C and 290 °C. As shown in Figs. 4–6, the DEAM fits well the instantaneous of V^r/V^* obtained by TG experiments in the temperature range of 240–290 °C, respectively, for xylan ($r^2 = 0.99$), lignin ($r^2 = 0.98$) and cellulose ($r^2 = 0.94$). In the case of cellulose (Fig. 6), the DAEM model slightly under-predicts the instantaneous V^r/V^* profiles at 250 °C and 270 °C while it shows small over-prediction at 280 °C and 290 °C. The optimum reaction orders for xylan, lignin and cellulose torrefaction reactions were 3, 2 and 1, respectively.

Fig. 7 shows the activation energy distribution of cellulose, xylan and lignin torrefaction reactions obtained using the log-normal distribution function. As can be seen, activation energy distributions of cellulose, xylan and lignin torrefaction reactions exhibit their respective maxima at 207 kJ/mol, 132 kJ/mol and 196 kJ/mol. In the case of cellulose and xylan, the activation energy distributions of the isothermal torrefaction reactions lie within the narrow ranges of 200–220 kJ/mol and 125–145 kJ/mol, respectively, showing that the parallel reactions involved in the cellulose and xylan torrefaction have close activation energies. Narrow ranges of activation energy distribution for non-isothermal pyrolysis of cellulose and hemicellulose have been already reported. Sonobe and Worasuwannarak [17] derived the distribution of activation energy for non-isothermal cellulose pyrolysis at temperatures as high as 600 °C and a narrow range of activation energy (180–190 kJ/mol) was reported with a maximum at 185 kJ/mol. Gasparovic et al. [57] also obtained an activation energy distribution for non-isothermal hemicellulose pyrolysis at temperatures as high as 500 °C using Gaussian distribution functions. They stated that the activation energy of hemicellulose pyrolysis is distributed in a range of 124–142 kJ/mol with a maximum at 132.9 kJ/mol. The narrow range of activation energy distribution for cellulose and xylan parallel torrefaction reactions suggests that a distributed activation energy model for xylan and cellulose torrefaction might be regarded as equivalent to that in which only one single reaction represents the overall cellulose and xylan torrefaction.

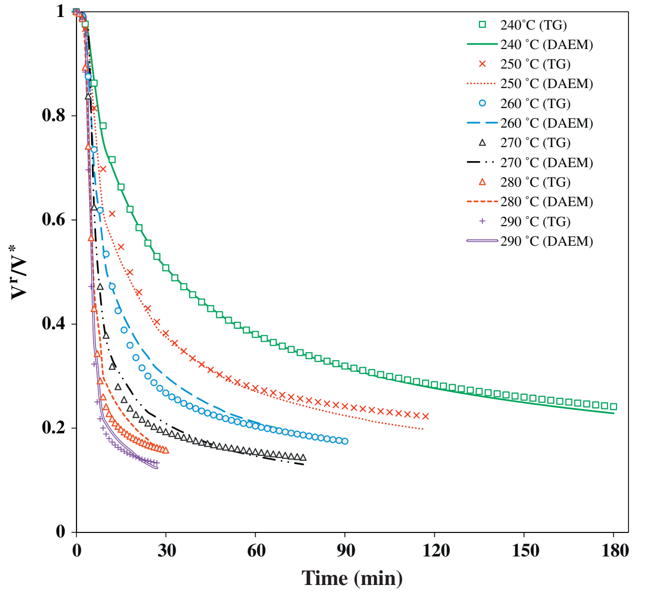

Fig. 4. TG derived profile of volatile release versus time for xylan torrefaction and DAEM simulated profiles of xylan torrefaction.

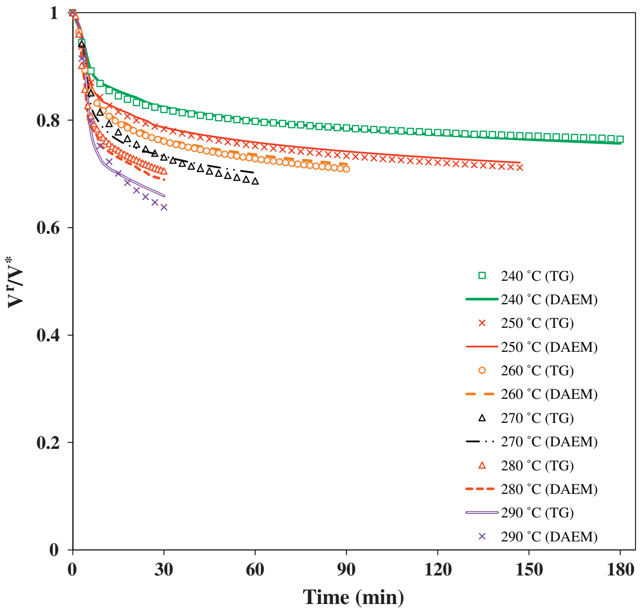

Fig. 5. TG derived profile of volatile release versus time for lignin torrefaction and the DAEM simulated profiles of lignin torrefaction.

In contrast to cellulose and xylan, the activation energy for the lignin torrefaction reactions is distributed widely in the range of 116–384 kJ/mol. This is in accordance with the wide activation energy distribution of Alcell lignin pyrolysis (129–361 kJ/mol) reported by Ferdous et al. [58] Mani et al. [33] also reported a wide

Table 3
Optimum values of parameters for the torrefaction kinetic models of cellulose, xylan, lignin, birch and aspen.

Biomass	E_0 (kJ/mol)	μ (kJ/mol)	δ (kJ/mol)	n	A_0 (min^{-1})	c_1	c_2	c_3	r^2
Xylan	89.8	3.76	0.05	3	1.815×10^{12}	...	...	...	0.99
Lignin	56.3	5.01	0.26	2	1.516×10^{16}	...	...	...	0.98
Cellulose	190.8	2.82	0.15	1	3.804×10^{17}	...	...	...	0.94
Aspen	...	...	...	...	...	0.534	0.235	0.231	0.97
Birch	...	...	...	...	...	0.584	0.212	0.204	0.97

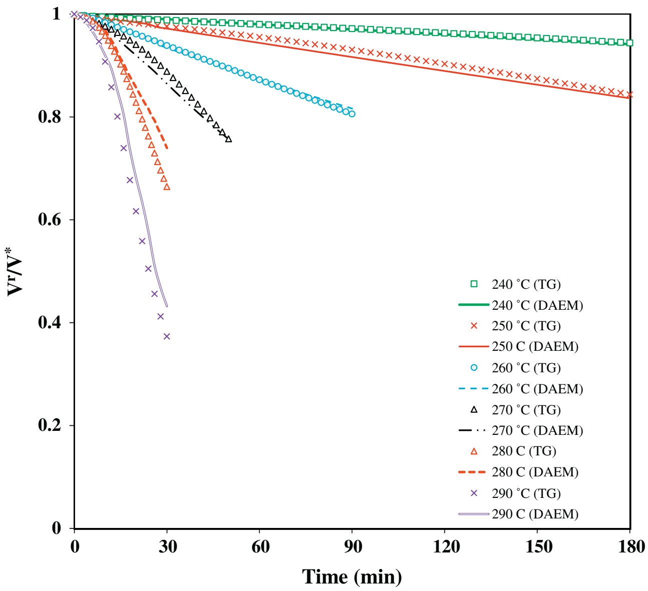

Fig. 6. TG derived profile of volatile release versus time for cellulose torrefaction and the DAEM simulated profiles of cellulose torrefaction.

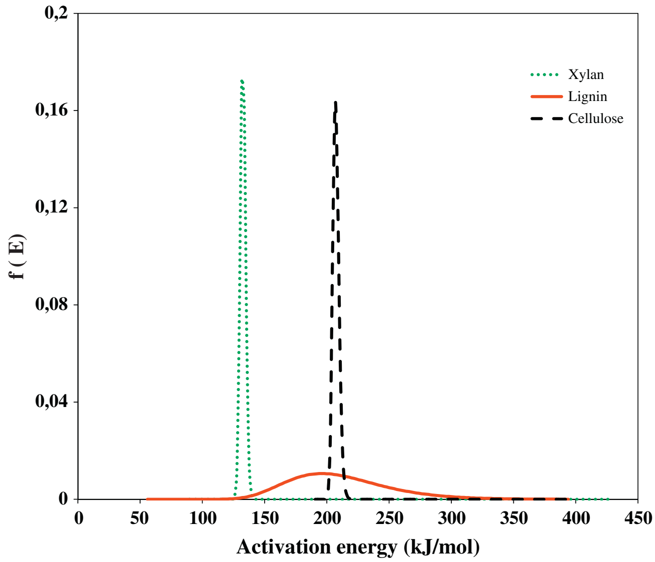

Fig. 7. Distributions of activation energies for xylan, cellulose and lignin.

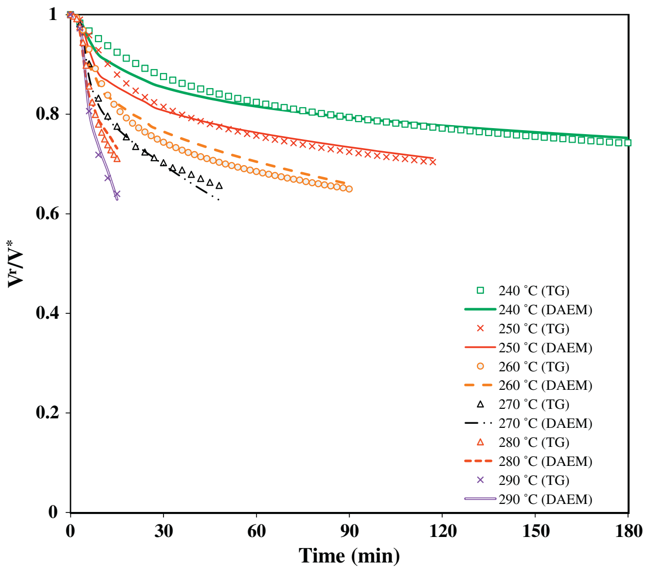

Fig. 8. TG derived profile of volatile release versus time for birch torrefaction and the simulated profiles using optimized c_i values.

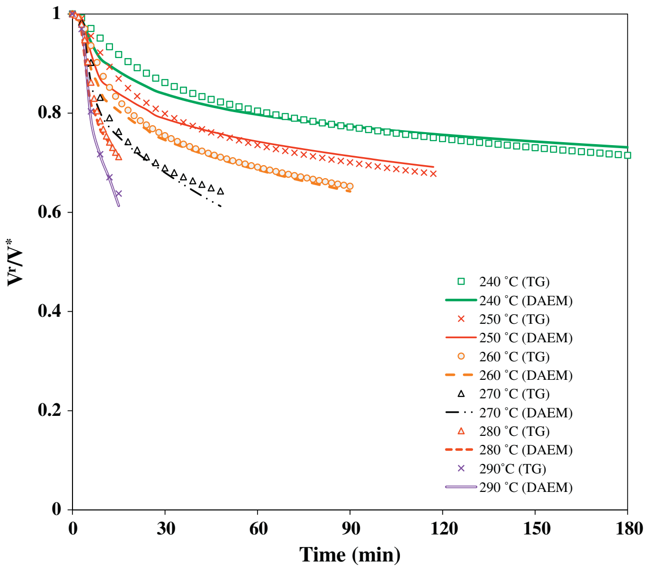

Fig. 9. TG derived profile of volatile release versus time for aspen torrefaction and the simulated trends using optimized c_i values.

range of activation energy for lignin pyrolysis (starting at around 100 kJ/mol) with maximum in the range of 158–170 kJ/mol. The broad activation energy revealed for lignin torrefaction could be due to the presence of various functional oxygen groups in the structure of lignin with different thermal stabilities leading to parallel reactions with broad activation energies. In addition, the presence of alkali and alkaline metals found in the structure of lignin could also catalyse some decomposition reactions during lignin torrefaction, shifting the activation energy distribution of lignin toward lower energies [17].

To formulate a model for predicting the extent of torrefaction of aspen and birch, it was assumed that their torrefaction is the result of independent torrefaction of their cellulose, hemicellulose and lignin content. Using the optimized value found for the DEAM of cellulose, xylan and lignin torrefaction, the contribution of each compound (c_i in Eq. (6)) was obtained so that the model best fits the TG derived V^r/V^* profile versus time at 240 °C, 260 °C and 280 °C. These values were used to predict the profile of V^r/V^* versus time for the torrefied birch and aspen at 250 °C, 270 °C and 290 °C. The model is in agreement with the experimental data within the temperature range from 240 °C to 290 °C as seen in Figs. 8 and 9 ($r^2 = 0.97$ for both aspen and birch torrefaction). The optimized values of cellulose, xylan and lignin contribution (c_i) on the volatile release of birch during its torrefaction are 0.584, 0.212 and 0.204, respectively. In the case of aspen wood, the contributions of the abovementioned compounds in the volatile release during torrefaction are 0.534, 0.235 and 0.231, respectively. Note that birch is composed of almost 58.9% of cellulose, 20.3% of hemicellulose and 20.8% of lignin [51] (values normalized on ash- and extractives-free basis). The computed contributions of each compound (c_i) on the volatile release of birch are close to the contributions of each compound in the chemical composition of birch wood. From this, it may be concluded that cellulose, xylan and lignin are decomposed independently during birch wood torrefaction

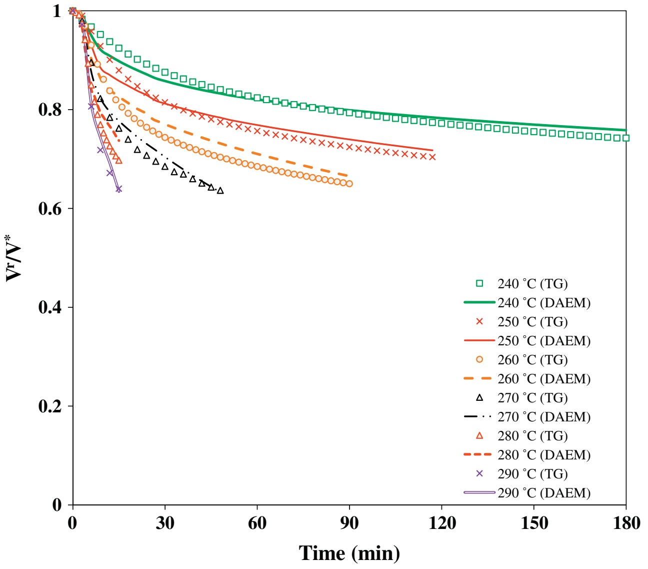

Fig. 10. TG derived profile of volatile release versus time for birch torrefaction and the results of its simulated profiles using the actual chemical composition of birch.

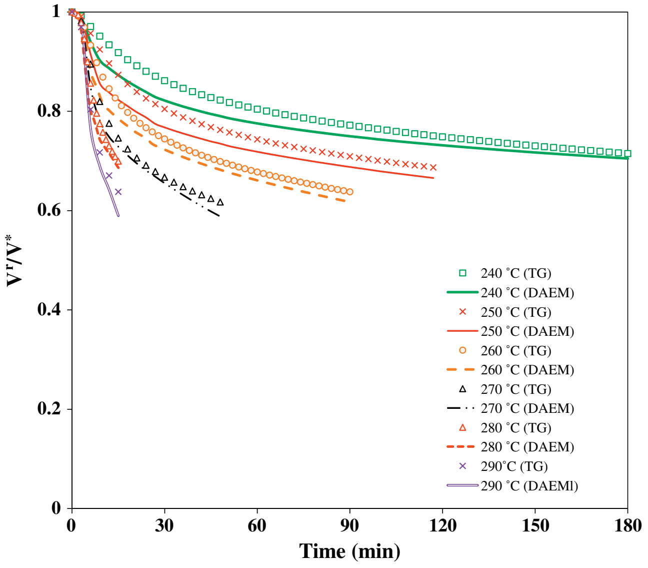

Fig. 11. TG derived profile of volatile release versus time for aspen torrefaction and the results of its simulated profiles using the actual chemical composition of aspen.

and the presence of alkali and alkaline metals mostly found in the lignin structure do not affect the rate of cellulose and hemicellulose torrefaction. As can be seen in Fig. 10, replacing c_i in Eq. (6) with the chemical composition of birch could fit well the experimentally obtained trends of V^r/V^* versus time at temperatures from 240–290 °C ($r^2 = 0.97$). However, in the case of aspen wood, the calculated values of c_i for cellulose, xylan and lignin were respectively, 4%, 15% and 8%, and different from their contributions in the chemical structure of aspen (51.2% of cellulose, 27.7% of hemicellulose and 21.1% of lignin [52]). Replacing c_i with the chemical composition of aspen leads to slight under-prediction of V^r/V^* versus time as shown in Fig. 11 ($r^2 = 0.92$). The difference between the chemical composition and the values obtained by the kinetic evaluation could be due to the effect of extractives decomposition on the torrefaction weight loss in the interrogated temperature range and/or to errors in the experimental techniques for obtaining the chemical composition of wood samples.

5. Conclusion

The torrefaction of two woody biomass samples (aspen and birch) and their main constituents (cellulose, xylan (representative of hemicellulose) and lignin) performed in a fixed-bed reactor showed that torrefaction improves the energy density of aspen and birch by reducing their oxygen and hydrogen content with respect to carbon in the solid residue. The equilibrium moisture content of birch and aspen and of their main constituents (cellulose, xylan and lignin) was reduced by about 30–40% due to torrefaction and was explained according to FTIR spectra to an ameliorated hydrophobicity upon torrefaction of the treated samples. Furthermore, the combined distributed activation energy model with a three-parameter log-normal distribution function could fit the experimental volatile release of xylan and lignin versus time while in the case of cellulose it exhibits some under-prediction. The distributed activation energy models developed for cellulose, xylan and lignin torrefaction could also be combined in three-parallel reaction meta-models for the kinetic description of aspen and birch torrefaction. The model could fit the experimental data of birch and aspen torrefaction in the mild and severe torrefaction conditions.

Acknowledgments

Support from the Natural Sciences and Engineering Research Council of Canada, the Canada Research Chair "Green processes for cleaner and sustainable energy", and the FQRNT-funded "Center in Green Chemistry and Catalysis" (CGCC) is gratefully acknowledged.

References

[1] G. Berndes, M. Hoogwijk, R. van den Broek, The contribution of biomass in the future global energy supply: a review of 17 studies, Biomass Bioenergy 25 (2003) 1–28.
[2] U. Arena, F. Di Gregorio, M. Santonastasi, A techno-economic comparison between two design configurations for a small scale, biomass-to-energy gasification based system, Chem. Eng. J. 162 (2010) 580–590.
[3] M.J.C. van der Stelt, H. Gerhauser, J.H.A. Kiel, K.J. Ptasinski, Biomass upgrading by torrefaction for the production of biofuels: a review, Biomass Bioenergy 35 (2011) 3748–3762.
[4] A. Pimchuai, A. Dutta, P. Basu, Torrefaction of agriculture residue to enhance combustible properties, Energy Fuels 24 (2010) 4638–4645.
[5] J. Deng, G.J. Wang, J.H. Kuang, Y.L. Zhang, Y.H. Luo, Pretreatment of agricultural residues for co-gasification via torrefaction, J. Anal. Appl. Pyrol. 86 (2009) 331–337.
[6] D. Medic, M. Darr, A. Shah, B. Potter, J. Zimmerman, Effects of torrefaction process parameters on biomass feedstock upgrading, Fuel 91 (2012) 147–154.
[7] S.K. Hoekman, A. Broch, C. Robbins, Hydrothermal carbonization (HTC) of lignocellulosic biomass, Energy Fuels 25 (2011) 1802–1810.
[8] W. Yan, J.T. Hastings, T.C. Acharjee, C.J. Coronella, V.R. Vasquez, Mass and energy balances of wet torrefaction of lignocellulosic biomass, Energy Fuels 24 (2010) 4738–4742.
[9] A. Sarvaramini, O. Gravel, F. Larachi, Torrefaction of ionic-liquid impregnated lignocellulosic biomass and its comparison to dry torrefaction, Fuel 103 (2013) 814–826.
[10] M. Atienza-Martinez, I. Fonts, J. Abrego, J. Ceamanos, G. Gea, Sewage sludge torrefaction in a fluidized bed reactor, Chem. Eng. J. 222 (2013) 534–545.
[11] J. Yu, C.B. Yao, X. Zeng, S. Geng, L. Dong, Y. Wang, S.Q. Gao, G.W. Xu, Biomass pyrolysis in a micro-fluidized bed reactor: Characterization and kinetics, Chem. Eng. J. 168 (2011) 839–847.
[12] M.J. Prins, K.J. Ptasinski, F. Janssen, Torrefaction of wood - Part 1. Weight loss kinetics, J. Anal. Appl. Pyrol. 77 (2006) 28–34.
[13] D. Klein-Marcuschamer, B.A. Simmons, H.W. Blanch, Techno-economic analysis of a lignocellulosic ethanol biorefinery with ionic liquid pre-treatment, Biofuels Bioprod. Biorefin. 5 (2011) 562–569.
[14] J.J. Chew, V. Doshi, Recent advances in biomass pretreatment -torrefaction fundamentals and technology, Renew. Sust. Energy Rev. 15 (2011) 4212–4222.
[15] V. Repellin, A. Govin, M. Rolland, R. Guyonnet, Modelling anhydrous weight loss of wood chips during torrefaction in a pilot kiln, Biomass Bioenergy 34 (2010) 602–609.
[16] J. Ratte, E. Fardet, D. Mateos, J.S. Hery, Mathematical modelling of a continuous biomass torrefaction reactor: TORSPYD (TM) column, Biomass Bioenergy 35 (2011) 3481–3495.

[17] T. Sonobe, N. Worasuwannarak, Kinetic analyses of biomass pyrolysis using the distributed activation energy model, Fuel 87 (2008) 414–421.

[18] L. Fiori, M. Valbusa, D. Lorenzi, L. Fambri, Modeling of the devolatilization kinetics during pyrolysis of grape residues, Bioresour. Technol. 103 (2012) 389–397.

[19] B. de Caprariis, P. De Filippis, C. Herce, N. Verdone, Double-Gaussian distributed activation energy model for coal devolatilization, Energy Fuels 26 (2012) 6153–6159.

[20] X.L. Liu, G. Pan, G. Wang, Z. Wen, Mathematical model of lump coal falling in the freeboard zone of the corex melter gasifier, Energy Fuels 25 (2011) 5729–5735.

[21] P. Tiwari, M. Deo, Detailed kinetic analysis of oil shale pyrolysis TGA data, AICHE J. 58 (2012) 505–515.

[22] J.J. Meng, J. Park, D. Tilotta, S. Park, The effect of torrefaction on the chemistry of fast-pyrolysis bio-oil, Bioresour. Technol. 111 (2012) 439–446.

[23] C.W. Wang, J.H. Peng, H. Li, X.T.T. Bi, R. Legros, C.J. Lim, S. Sokhansanj, Oxidative torrefaction of biomass residues and densification of torrefied sawdust to pellets, Bioresour. Technol. 127 (2013) 318–325.

[24] W.H. Chen, H.C. Hsu, K.M. Lu, W.J. Lee, T.C. Lin, Thermal pretreatment of wood (Lauan) block by torrefaction and its influence on the properties of the biomass, Energy 36 (2011) 3012–3021.

[25] A. Friedl, E. Padouvas, H. Rotter, K. Varmuza, Prediction of heating values of biomass fuel from elemental composition, Anal. Chim. Acta 544 (2005) 191–198.

[26] T.G. Bridgeman, J.M. Jones, I. Shield, P.T. Williams, Torrefaction of reed canary grass, wheat straw and willow to enhance solid fuel qualities and combustion properties, Fuel 87 (2008) 844–856.

[27] T.G. Bridgeman, J.M. Jones, A. Williams, D.J. Waldron, An investigation of the grindability of two torrefied energy crops, Fuel 89 (2010) 3911–3918.

[28] R. Radmanesh, Y. Courbariaux, J. Chaouki, C. Guy, A unified lumped approach in kinetic modeling of biomass pyrolysis, Fuel 85 (2006) 1211–1220.

[29] J.M. Cai, R.H. Liu, New distributed activation energy model: Numerical solution and application to pyrolysis kinetics of some types of biomass, Bioresour. Technol. 99 (2008) 2795–2799.

[30] B. Jankovic, The comparative kinetic analysis of Acetocell and Lignoboost (R) lignin pyrolysis: the estimation of the distributed reactivity models, Bioresour. Technol. 102 (2011) 9763–9771.

[31] J.M. Cai, R.H. Liu, Parametric study of the nonisothermal nth-order distributed activation energy model involved the Weibull distribution for biomass pyrolysis, J. Therm. Anal. Calorim. 89 (2007) 971–975.

[32] B. Jankovic, Identification of the effective distribution function for determination of the distributed activation energy models using Bayesian statistics: application of isothermal thermogravimetric data, Int. J. Chem. Kinet. 42 (2010) 641–658.

[33] T. Mani, P. Murugan, N. Mahinpey, Determination of distributed activation energy model kinetic parameters using simulated annealing optimization method for nonisothermal pyrolysis of lignin, Ind. Eng. Chem. Res. 48 (2009) 1464–1467.

[34] D. Saxena, G. Stotzky, Bt corn has a higher lignin content than non-Bt corn, Am. J. Bot. 88 (2001) 1704–1706.

[35] Q. Liu, S.R. Wang, Y. Zheng, Z.Y. Luo, K.F. Cen, Mechanism study of wood lignin pyrolysis by using TG-FTIR analysis, J. Anal. Appl. Pyrol. 82 (2008) 170–177.

[36] M.P. Pandey, C.S. Kim, Lignin depolymerization and conversion: a review of thermochemical methods, Chem. Eng. Technol. 34 (2011) 29–41.

[37] H. Pinkowska, P. Wolak, A. Zlocinska, Hydrothermal decomposition of alkali lignin in sub- and supercritical water, Chem. Eng. J. 187 (2012) 410–414.

[38] S. Kubo, J.F. Kadla, Hydrogen bonding in lignin: a Fourier transform infrared model compound study, Biomacromolecules 6 (2005) 2815–2821.

[39] V.D. Barrera-Garcia, D. Chassagne, C. Paulin, J. Raya, J. Hirschinger, A. Voiley, J.P. Bellat, R.D. Gougeon, Interaction mechanisms between guaiacols and lignin: the conjugated double bond makes the difference, Langmuir 27 (2011) 1038–1043.

[40] I.M. Saxena, R.M. Brown, Cellulose biosynthesis: current views and evolving concepts, Ann Bot. – London 96 (2005) 9–21.

[41] E. Hoekstra, W.P.M. Van Swaaij, S.R.A. Kersten, K.J.A. Hogendoorn, Fast pyrolysis in a novel wire-mesh reactor: decomposition of pine wood and model compounds, Chem. Eng. J. 187 (2012) 172–184.

[42] J. Scheirs, G. Camino, W. Tumiatti, Overview of water evolution during the thermal degradation of cellulose, Eu. Polym. J. 37 (2001) 933–942.

[43] Y.C. Lin, J. Cho, G.A. Tompsett, P.R. Westmoreland, G.W. Huber, Kinetics and mechanism of cellulose pyrolysis, J. Phys. Chem. C 113 (2009) 20097–20107.

[44] C. Schadel, A. Richter, A. Blochl, G. Hoch, Hemicellulose concentration and composition in plant cell walls under extreme carbon source-sink imbalances, Physiol. Plant. 139 (2010) 241–255.

[45] F. Peng, P. Peng, F. Xu, R.C. Sun, Fractional purification and bioconversion of hemicelluloses, Biotechnol. Adv. 30 (2012) 879–903.

[46] Y. Arslan, S. Takac, N. Eken-Saracoglu, Kinetic study of hemicellulosic sugar production from hazelnut shells, Chem. Eng. J. 185 (2012) 23–28.

[47] C. Schadel, A. Bochl, A. Richter, G. Hoch, Quantification and monosaccharide composition of hemicelluloses from different plant functional types, Plant Physiol. Biochem. 48 (2010) 1–8.

[48] D.K. Shen, S. Gu, A.V. Bridgwater, Study on the pyrolytic behaviour of xylan-based hemicellulose using TG-FTIR and Py-GC-FTIR, J. Anal. Appl. Pyrol. 87 (2010) 199–206.

[49] I. Spiridon, P. Valentin, Polysaccharides Structural Diversity and Functional Versatility, second ed., 2004.

[50] R.K. Sharma, J.B. Wooten, V.L. Baliga, M.R. Hajaligol, Characterization of chars from biomass-derived materials: pectin chars, Fuel 80 (2001) 1825–1836.

[51] C. Li, M. Zheng, A. Wang, T. Zhang, On-pot catalytic hydrocracking of woody biomass into chemicals over supported carbide catalysts: simultaneous conversion of cellulose, hemicellulose and lignin, Energy Environ. Sci. (2011).

[52] G. Chauvette, M. Heitz, M. Rubio, J. Khorami, E. Chornet, H. Menard, TG–DTG as a rapid method for the characterization of solid residues derived from liquefaction of lignocellulosics, Thermochim. Acta 84 (1985) 1–5.

[53] C.P. Hoang, K.A. Kinney, R.L. Corsi, P.J. Szaniszlo, Resistance of green building materials to fungal growth, Int. Biodeterior. Biodegrad. 64 (2010) 104–113.

[54] P. Verma, J. Dyckmans, H. Militz, C. Mai, Determination of fungal activity in modified wood by means of micro-calorimetry and determination of total esterase activity, Appl. Microbiol. Biotechnol. 80 (2008) 125–133.

[55] C.G. Carll, T.L. Highley, Decay of wood and wood-based products above ground in buildings, J. Test. Eval. 27 (1999) 150–158.

[56] D.B. Sauer, Effects of fungal deterioration on grain - nutritional-value, toxicity, germination, Int. J. Food. Microbiol. 7 (1988) 267–275.

[57] L. Gasparovic, J. Labovsky, J. Markos, L. Jelemensky, Calculation of kinetic parameters of the thermal decomposition of wood by distributed activation energy model (DAEM), Chem. Biochem. Eng. Q. 26 (2012) 45–53.

[58] D. Ferdous, A.K. Dalai, S.K. Bej, R.W. Thring, Pyrolysis of lignins: experimental and kinetics studies, Energy Fuels 16 (2002) 1405–1412.